Electronic Supplementary Material (ESI) for Nanoscale.

Supplementary Information

Enhanced water vapor separation by temperature-controlled aligned-multiwalled carbon nanotube membranes

Wonjae Jeon,[a] *Jongju Yun,*[a] *Fakhre Alam Khan,*[b] *Seunghyun Baik*[*b,c]

[a]Department of Energy Science, Sungkyunkwan University, Suwon 440-746, Korea.

[b]School of Mechanical Engineering, Sungkyunkwan University, Suwon 440-746, Korea.

[c]Center for Integrated Nanostructure Physics, Institute for Basic Science (IBS), Sungkyunkwan University, Suwon 440-746, Korea

*To whom correspondence should be addressed. E-mail: sbaik@me.skku.ac.kr

Intertube distance of aligned-MWNTs

The nanotube areal density (1.9×10^{10} cm^{-2}) was calculated using the weight and size information of aligned-MWNTs using a previously published protocol.[S1, S2] The total number of nanotubes (N_{tubes}) was 4.75×10^9 when the area of silicon wafer was 5 x 5 mm^2. The intertube distance was then calculated assuming square array of nanotubes.[S1, S2]

$$\text{Intertube distance} = \sqrt{\frac{A}{N_{\text{tubes}}}} \qquad \text{(S1)}$$

where A is the area of aligned-MWNTs. The average intertube distance of aligned-MWNTs was 73 nm when the area was 5 x 5 mm^2.[S1, S2] The average intertube distance of aligned-MWNTs was 15 nm when the area was 1 x 1 mm^2 after the squeezing process shown in Fig. 3a.

Correction factor for the flow meter

A rotary-type flow meter calibrated with N_2 by the supplier (Unicell, IF-K, 0.3 - 10 sccm) was used to monitor the gas flow rate. The correction factor was calculated for different gas species using a previously published method.[S1, S2, S3]

$$Q_{\mathrm{gas}} = \sqrt{\frac{M_{\mathrm{N_2}}}{M_{\mathrm{gas}}}} \cdot Q_{\mathrm{measured}} \qquad \text{(S2)}$$

where Q_{gas} is the corrected flow rate of each gas, $M_{\mathrm{N_2}}$ is the molecular weight of N_2, M_{gas} is the molecular weight of gas, and Q_{measured} is the measured flow rate. The molecular weight of helium was used for the calibration of helium-water vapor binary gas mixtures since the mole fraction of water vapor was small.[S1, S2]

Aligned-MWNTs before and after the water vapor separation experiments

There was no change in aligned structure of carbon nanotubes before and after the repeated water vapor separation experiments.

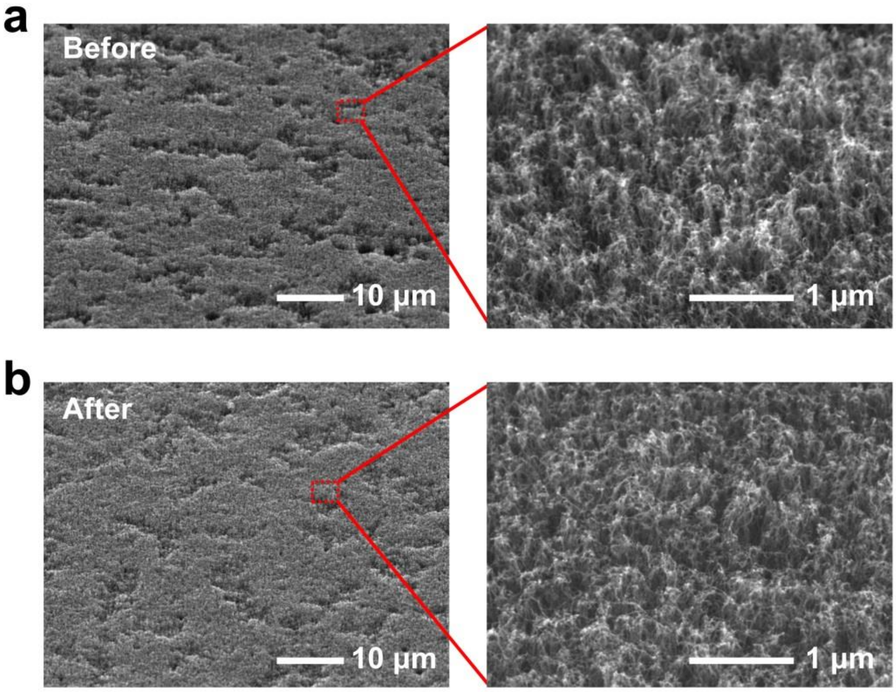

Fig. S1. SEM images of aligned-MWNTs before (a) and after (b) the water vapor separation experiments. Aligned-MWNTs were tilted at 45°, and top surface was imaged by SEM.

Comparison of helium-water vapor and nitrogen-water vapor mixture transports through aligned-MWNTs.

Fig.S2 compares helium-water vapor and nitrogen-water vapor mixture transports through aligned-MWNTs under the identical pressure drop (3.4~3.5 kPa) across the membrane. The membrane temperature was 5 ^{o}C. The feed-side RH was kept high (>90%). The permeate-side RH was similar for both binary gas mixtures.

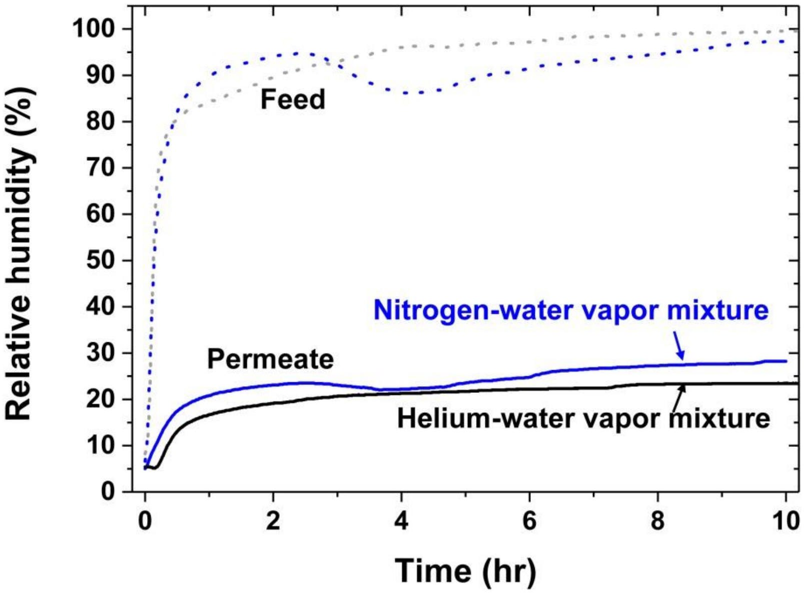

Fig. S2. Comparison of helium-water vapor and nitrogen-water vapor mixture transports through aligned-MWNTs. The membrane temperature was 5°C. The helium-water vapor mixture transport data were reproduced from Fig. 2a for comparison.

Mass flow rate estimation of water vapor and helium

The mass flow rate of water vapor and helium was estimated using a previously published protocol and briefly summarized below.[S1, S2] An ideal gas mixture was assumed where the total pressure is equal to the sum of partial pressure of each component (Dalton's assumption).[S4]

$$P_{\mathrm{t-feed}} = P_{\mathrm{w-feed}} + P_{\mathrm{He-feed}} \tag{S3}$$

$$P_{\mathrm{t-permeate}} = P_{\mathrm{w-permeate}} + P_{\mathrm{He-permeate}} \tag{S4}$$

where P_{t}, P_{w}, and P_{He} are the total pressure, water vapor pressure, and helium partial pressure, respectively. Subscripts 'feed' and 'permeate' refer to the feed and permeate side. $P_{\mathrm{w-feed}}$ and $P_{\mathrm{w-permeate}}$ were calculated using the measured RH, temperature, P_{t}, and psychrometric chart. The mass flow rate ($\dot{m}$) of water vapor and helium was then calculated using follow equations.

$$\dot{m}_{\mathrm{w-feed}} = \frac{P_{\mathrm{w-feed}} \cdot \dot{V}_{\mathrm{feed}} \cdot M_{\mathrm{w}}}{R \cdot T} \tag{S5}$$

$$\dot{m}_{\mathrm{He-feed}} = \frac{P_{\mathrm{He-feed}} \cdot \dot{V}_{\mathrm{feed}} \cdot M_{\mathrm{He}}}{R \cdot T} \tag{S6}$$

$$\dot{m}_{\mathrm{w-permeate}} = \frac{P_{\mathrm{w-permeate}} \cdot \dot{V}_{\mathrm{permeate}} \cdot M_{\mathrm{w}}}{R \cdot T} \tag{S7}$$

$$\dot{m}_{\mathrm{He-permeate}} = \frac{P_{\mathrm{He-permeate}} \cdot \dot{V}_{\mathrm{permeate}} \cdot M_{\mathrm{He}}}{R \cdot T} \tag{S8}$$

where $\dot{V}$ is the volume flow rate, M is the molar mass, R is the ideal gas constant, and T is the temperature. $\dot{V}_{\mathrm{permeate}}$ was measured by the flow meter. The mass flow rate of helium was assumed to be conserved on both feed and permeate sides due to the helium's chemical inertness and non-adsorbing nature to carbonaceous materials.[S1, S2, S5]

$$\dot{m}_{\mathrm{He-feed}} = \dot{m}_{\mathrm{He-permeate}} \tag{S9}$$

Finally, $\dot{V}_{\mathrm{feed}}$ and $\dot{m}_{\mathrm{w-feed}}$ were obtained from Equations S5 and S6.[S1, S2]

Continuum finite element simulation of gas temperature

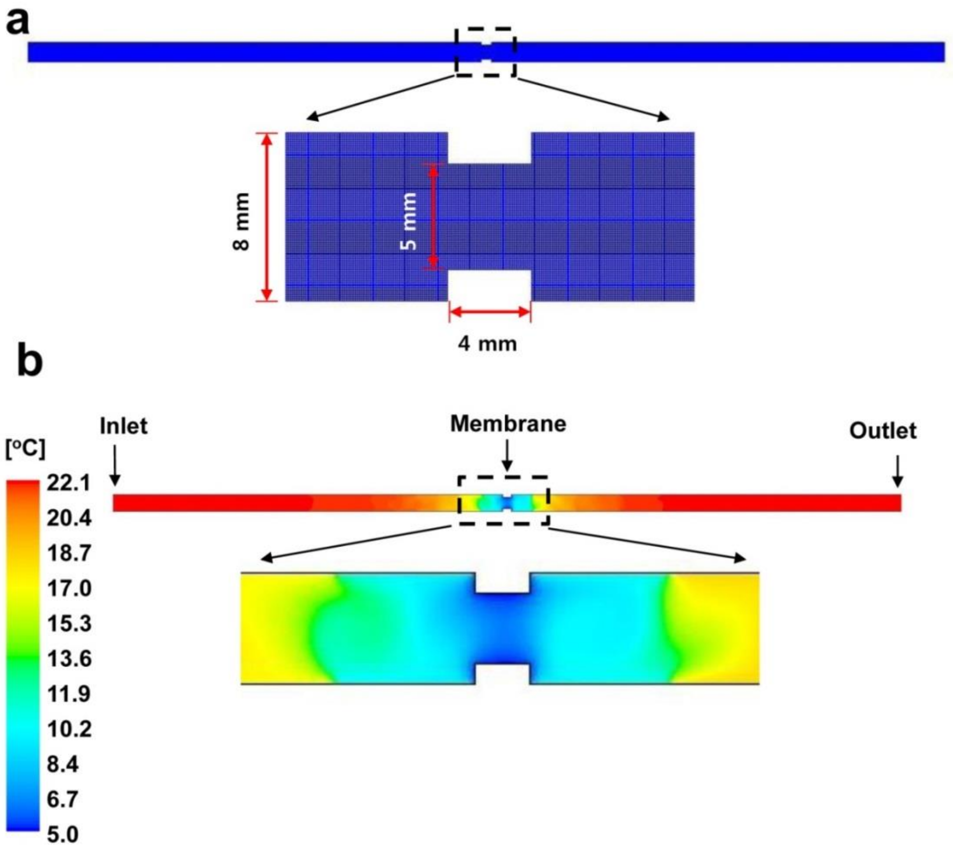

Fig. S3. **Finite element simulation.** (a) Grid construction of the channel. (b) Simulated helium temperature distribution.

The helium temperature distribution along the tube and membrane channel was simulated using the continuum finite element method (Fluent). For simplicity, the individual nanotube geometry inside the membrane channel and water vapor were not considered in the simulation. The 2-dimensional channel geometry and generated mesh are shown in Fig. S3a. The tube length (18 cm) before and after the constricting channel section (4 mm) was long enough to have fully developed flow at the inlet and outlet planes. Quadrilateral meshes were constructed by ANSYS Workbench Design Modeller.[S6] The numbers of elements and nodes were 290,000 and 293,751. The ideal gas model was selected for helium gas, and no-slip condition was used for the wall. The inlet velocity, inlet gauge pressure, and outlet gauge pressure were set at 2.24 x 10^{-3} m/s, 3,710 Pa, and 330 Pa reflecting the experimental conditions. The tube wall temperature was experimentally measured and used as a constant temperature boundary condition with regard to time (Table S1). The simulated helium temperature is shown in Fig. S3b.

Channel side	Distance from the membrane (cm)	Temperature (°C)
Feed	18	22.1
	17	22.1
	16	22.1
	15	22.1
	14	22.1
	13	22.1
	12	22
	11	22
	10	22
	9	21.9
	8	21.9
	7	21.8
	6	21.7
	5	21.4
	4	20.4
	3	19.3
	2	17.1
	1	9.7
Membrane channel	0	5
Permeate	1	9.9
	2	18.3
	3	20
	4	20.9
	5	21.3
	6	21.9
	7	21.9
	8	22
	9	22
	10	22
	11	22
	12	22.1
	13	22.1
	14	22.1
	15	22.1
	16	22.1
	17	22.1
	18	22.1

Table S1. Experimentally measured wall temperature.

Water vapor transports through PTFE and PC membranes

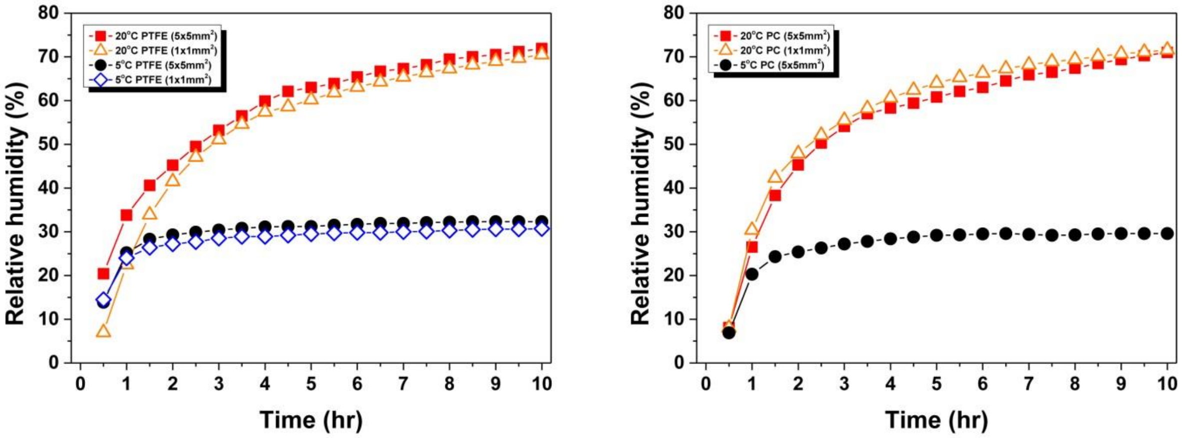

Fig. S4. Comparison of water vapor transports through polymer membranes with two different flow areas (5 x 5 mm^2 and 1 x 1 mm^2) (a) PTFE membrane. (b) PC membrane.

Polymer membranes with two different flow areas (5 x 5 mm^2 and 1 x 1 mm^2) were employed for helium-water vapor transport experiments. The flow area of aligned-MWNTs with an intertube distance of 73 nm was 5 x 5 mm^2, and that of aligned-MWNTs with an intertube distance of 15 nm was 1 x 1 mm^2. The experiments were carried out under the identical flow rate (6.88 sccm). As shown in Fig. S4a, there was no significant difference in permeate-side RH for hydrophobic PTFE membranes with different flow areas both at 20 and 5 ^{o}C. The permeate-side RH was also similar for hydrophilic PC membranes with different flow areas at 20 ^{o}C (Fig. S4b). However, at the membrane temperature of 5 ^{o}C, the hydrophilic PC membrane with an area of 1 x 1 mm^2 was completely wet with the condensed water resulting in an increase in feed-side pressure and leaking in the tubing system. Therefore, the permeate-side RH could not be measured for the PC membrane.

REFERENCES

S1. J. Yun, W. Jeon, F. A. Khan, J. Lee and S. Baik, *Nanotechnology*, 2015, **26**, 235701.

S2. D. Yoon, C. Lee, J. Yun, W. Jeon, B. J. Cha and S. Baik, *ACS Nano*, 2012, **6**, 5980-5987.

S3. E. Ower and R. C. Pankhurst, *The Measurement of Air Flow*, Elsevier Science, 2014.

S4. Y. Cengel and M. Boles, *Thermodynamics: An Engineering Approach*, McGraw-Hill Education, New York, USA, 2014.

S5. R. Ash, R. Baker and R. Barrer, *Proc. R. Soc. London, Ser. A*, 1967, **299**, 434-454.

S6. P. L. Baehmann, S. L. Wittchen, M. S. Shephard, K. R. Grice and M. A. Yerry, *Int. J. Numer. Meth. Eng.*, 1987, **24**, 1043-1078.